Analytical Methods

ROYAL SOCIETY OF CHEMISTRY

PAPER

View Article Online
View Journal

Cite this: DOI: 10.1039/d1ay00945a

A new and high-performance microfluidic analytical device based on Fusion 5 paper for the detection of chili pepper anthracnose pathogen *Colletotrichum truncatum*†

Amir Osman Abdelrazig,[a] Bao Thai Tran,[a] Patsamon Rijiravanich *[b] and Werasak Surareungchai*[ac]

A microfluidic analytical device based on wax-patterned Fusion 5 paper was designed and fabricated to facilitate early detection and improve control of anthracnose disease. Here, a rapid, specific, on-site, and low operational cost nucleic acid biosensor (ACT-Ct-PAD) based on the actin gene (ACT) and wax-patterned Fusion 5 paper was used to detect the PCR products of *Colletotrichum truncatum* (Ct), the main causal agent of chili anthracnose in Asia. The sensor was developed by using DNA conjugated gold nanoparticles (AuNPs-DNA) as a detection probe, which will hybridize to a complementary target sequence. Avidin coated mesoporous silica particles were attached to biotin-tagged DNA sequences forming capture probes, which were immobilized on the test and control zones of the device. The hybridization complex (MSP-dsDNA-AuNPs) produces an intense red color, which provides a platform for colorimetric detection. By targeting an actin gene sequence, the ACT-Ct-PAD device allows the detection of Ct DNA within 15 min. The specificity of the sensor was confirmed by the absence of a positive signal for DNA from non-target *Colletotrichum* species and two different fungal genera. Our wax-patterned Fusion 5 sensor provides a simple tool for the rapid nucleic acid diagnosis with a detection limit down to 17.42 femtomoles. This method has the potential to be applied for protein assay as well; hence, it has a considerable impact on on-site diagnostics.

Received 3rd June 2021
Accepted 1st July 2021

DOI: 10.1039/d1ay00945a

rsc.li/methods

Introduction

Anthracnose of chili (*Capsicum annum* L.) is one of the most devastating diseases causing major production losses and reducing the marketability of the fruit. Chili anthracnose has been shown to be caused by 24 species of the genus *Colletotrichum*, which belongs to the kingdom fungi and classified as one of the top 10 fungal pathogen groups in molecular plant pathology.[1] In Asia, *Colletotrichum truncatum* (*C. truncatum*) is the most prevalent species of *Colletotrichum* causing anthracnose of chili.[2] Accurate detection of *Colletotrichum* species is a pre-requisite for disease management and implementation of control strategies. The standard blotter test is often used for the detection of *Colletotrichum* species in chili seed samples according to the International Seed Testing Association (ISTA). However, these methods are time consuming, tedious and require extensive taxonomic knowledge. Molecular techniques especially those based on the polymerase chain reaction (PCR) have become useful to develop more specific and sensitive detection methods.[3–5] Although they have a number of advantages over other classical techniques, they still have some limitations as they use expensive equipment and require a skilled operator. Alternatively, fungal pathogens can be detected by other molecular techniques such as loop-mediated isothermal amplification[6] and PCR-nucleic acid lateral flow immunoassay.[7]

There are several DNA regions targeted for the identification of *Colletotrichum* species such as the nuclear rDNA internal transcribed spacer (ITS)[8,9] and protein coding genes.[10,11] The most commonly used DNA region to design primers for PCR-based identification and detection of plant pathogenic fungi is the ITS.[12] Despite the wide spread usage of this region as a fungal identification code, it still has many limitations.[13] On the other hand, actin is a protein coding gene used to reclassify the genus *Colletotrichum* and contains more phylogenetic

[a]*School of Bioresources and Technology, King Mongkut's University of Technology Thonburi, Bang Khun Thian, Bangkok 10150, Thailand*

[b]*BioSciences and Systems Biology Research Team, National Center for Genetic Engineering and Biotechnology, National Sciences and Technology Development Agency at King Mongkut's University of Technology Thonburi, Bang Khun Thian, Bangkok 10150, Thailand. E-mail: patsamon.rij@biotec.or.th*

[c]*Nanoscience and Nanotechnology Graduated Research Program, Faculty of Science, King Mongkut's University of Technology Thonburi, Bangmod, Bangkok 10140, Thailand. E-mail: werasak.sur@kmutt.ac.th*

† Electronic supplementary information (ESI) available. See DOI: 10.1039/d1ay00945a

information compared to the ITS region; hence, it is an ideal marker to differentiate closely related species.[14] Moreover, the sequences of this gene are easy to amplify and align,[15,16] allowing the study of relationships and variation in the species.

A simple, rapid, cost-effective, and decentralized test is required for early detection and screening of *Colletotrichum* species from fruit tissues and seed samples. Recently, microfluidic devices made using paper have gained considerable interest, as the fluid flow through the paper can be controlled by the fabrication of hydrophobic wax barriers. Preparation of such barriers can be performed *via* wax printing using a wax printer, which is proved to be a simple and cost-effective method. The main advantage of a paper-based microfluidic device is that it provides a user-friendly, cost-effective, simple, rapid and portable diagnostic tool for the end user.[17–21] The major applications of paper-based microfluidics are medical diagnostics, environmental monitoring, and food quality control.[22] To detect the analytes in these potential areas, suitable transduction techniques need to be developed and optimized, such as colorimetric,[23–25] electrochemical,[26,27] chemiluminescence,[28,29] electrochemiluminescence,[30–33] and fluorescence[34,35] techniques.

Various types of paper have been applied to design a wide range of bio-sensing platforms.[36] Among these, porous cellulose is the most widely used commercial material in a majority of these designs. The cellulose chemical structure contains an abundance of hydroxyl groups (–OH), which are not highly reactive; therefore, in most cases, surface modification is required to modulate the functional nature of the paper materials.[22,37] However, surface modification may affect the natural characteristics of the paper materials.[22] This may make their application difficult for specific types of bio-diagnostic platforms.[38] Furthermore, even if the properties of the paper are not affected by modification techniques, it still might not be possible to carefully control the generation of active functional groups and their even distribution on the paper surface.[39,40] Optimal generation and distribution of the surface functional groups are crucial for biomolecule immobilization and subsequent detection of the analyte of interest. In this context, a glass fiber-based material called Fusion 5 with a thickness of 0.37 nm, capillary flow rate of 38 s/4 cm, and particle retention size of 2.3 μm, can overcome these problems. Unlike cellulose and nitrocellulose, Fusion 5 paper is non-protein and non-conjugate binding. This anti-fouling property is attributed to the fact that Fusion 5 paper does not support electrostatic and hydrophobic interactions with proteins.[41,42]

Herein, we developed a single paper lateral flow assay for the detection of *C. truncatum* nucleic acid, using the actin gene sequence. The design and fabrication of the wax-patterned Fusion 5 sensor (ACT-Ct-PAD) was performed and the colorimetric signal obtained from the *C. truncatum* target DNA was quantified by grey intensity measurements. To the best of our knowledge this is the first report of using Fusion 5 paper to design a nucleic acid-based microfluidic device. It offers a simple platform which circumvents the use of tedious blocking and other modification steps, normally applied to other types of paper.[43,44] Moreover, the paper cost is lower than that of a nitrocellulose membrane but higher than that of cellulose paper; however, cellulose paper requires modifications which will probably increase the cost.[41]

Materials and methods

Materials

All chemicals used in this work were of analytical reagent grade and were used as received. Avidin from egg white (Cat. no. A9275), gold(III) chloride trihydrate (Cat. no. 520918), poly(-allylamine hydrochloride) (PAA, $M_W \sim 17\,500$; Cat. no. 283215), poly(sodium 4-styrenesulfonate) (PSS, $M_W \sim 7000$; Cat. no. 243051), tris(2-carboxyethyl) phosphine (TCEP; Cat. no. 646547), tetraethyl orthosilicate (TEOS; Cat. no. 86578), and Tween-20 (Cat. no. P1379) were purchased from Sigma-Aldrich. Tris(hydroxymethyl)aminomethane (Cat. no. 1.08382) was purchased from Merck (Germany). Sucrose (Cat. no. SB0498) and cetyltrimethylammonium bromide (CTAB; Cat. no. CB0108) were purchased from Bio Basic Inc (Canada). Sodium borate and potassium chloride were purchased from Ajax Finechem (Australia). Sodium chloride was purchased from CARLO ERBA Reagents (Cat. no. 479687). Phosphate buffered saline (1× PBS, 10 mM $Na_2HPO_4 \cdot 7H_2O$, 1.8 mM KH_2PO_4, 137 mM NaCl and 2.7 mM KCl), pH 7.4, was used for the preparation of the MSP-capture probe and detection on the PAD. All solutions and buffers were prepared using Type 2 pure water or higher quality from Merck Millipore (USA and Canada).

Fusion 5 paper (Cat. no. 8151-6755) was purchased from Whatman (Germany). The transparent film (Product code 419414010) was obtained from Hi-jet (Thailand). The customized nucleotide probes, primers, and target DNAs used in this study were purchased from Integrated DNA Technologies Pte. Ltd. (Singapore) and their sequences were shown in Table 1. The location of the primers and probes relative to the sequence of the actin gene of *Colletotrichum truncatum* (accession no. L170499), was presented in Fig. S1.†

All *Colletotrichum* isolates in this study were obtained from the Department of Plant Pathology, Faculty of Agriculture, Kasetsart University. They were isolated from chili fruits with anthracnose symptoms collected from chili producing fields.

Apparatus

Inkscape 0.91 software was used to design the patterns, which were printed onto a transparent film using a wax printer (Xerox ColorQube 8880) with a Fuji Xerox solid black ink stick (Cat. no. 108R00945). Photos of the device were captured using a 12.2 MP and resolution 768 by 1024 pixels smartphone camera (Apple-iPhone-x). ImageJ software, v. 1.50i, (National Institutes of Health Bethesda, Md, USA) was used for image analysis and quantification of signal intensities.

Preparation of infected chili seeds

Chili seeds were artificially infected with a *Colletotrichum* spore suspension to mimic the real samples of infected chili seeds. The spore suspension was prepared from a 9 day old culture by adding 10 mL of sterilized distilled water to the plate. The

Table 1 Nucleotide sequences used in this study[a]

Name	Sequence (5′-3′)
Test Rp (Ct)	SS-$(CH_2)_6$-GGG ATG GAT AAC CGG AA
Test Cp (Ct)	GTC TGT GTG TGG GTG GTA GA-biotin
Blocking probe	SS-$(CH_2)_6$-TTT TTT TTT
Control Rp	SS-$(CH_2)_6$-TAA GCA ACC GAT CAA GT
Control Cp	ACT TGA TCG GTT GCT TA-biotin
Ct-tDNA	TCT ACC ACC CAC ACA CAG ACC GCA ATC TTG CCC GTC AGG GGC TAT CGA GAT TTC CGG TTA TCC ATC CC
Ct-Fw primer	TCT ACC ACC CAC ACA CAG AC
Ct-Rv primer	GCG AGA TGG TTA GCA TTG A
Cs-tDNA	TGC GCC CAG AGC TGT CTT CCG TAA GTT CCC CAT CAT CCG CAG ACC GCA AT
Cg-tDNA	CCT CCAT CGT CGG TCG CCC TCG CCA CCA TGG GTA TGT CTG CTT CTC
Aspergillus niger	AAT TCA GTG AAT CAT CGA GTC TTT GAA CGC ACA TTG CGC CCC CTG GCA TT
Alternaria alternata	GTG TGA ATT GCA GAA TTC AGT GAA TCA TCG AAT CTT TGA ACG CAC ATT GC

[a] *(Rp = reporter probe, Cp = capture probe, t-DNA = target DNA, Fw = forward, Rv = reverse, Ct = *C. truncatum*, Cs = *C. scovillei*, and Cg = *C. gloeosporioides*).

suspension was filtered through sterile cheesecloth and then adjusted to 1×10^4 spore per mL. Sterilized healthy chili seeds were inoculated by spraying the spore suspension at 5 mL per 800 chili seeds in sterile plastic bags. The inoculated seeds were incubated overnight at 25 °C, air dried in a laminar flow and kept at 4 °C for further use.

Preparation of the AuNP-DNA label

AuNPs were synthesized through citrate reduction of $HAuCl_4$. Briefly, 100 mL of 1 mM $HAuCl_4$ was heated to boiling under vigorous stirring, and then, 10 mL of 38.8 mM sodium citrate was quickly added to the reaction mixture. The color of the solution changes from pale yellow to wine red in 2 min. After that, the solution was kept boiling under stirring for an additional 10 min to ensure complete reduction. The optical density (OD) of the AuNPs was determined at a peak wavelength of 520 nm. The synthesized AuNPs were stored at 4–6 °C. For the preparation of the AuNPs-nucleotide conjugate, 45 μL of a mixture of 100 μM thiolated oligonucleotides (detection probe, control reporter probe, and blocking probe) with a volume ratio of 3 : 1 : 0.5 were used to conjugate with AuNPs. Prior to use, the disulfide groups on the DNA were cleaved by the addition of 1 μL of 10 mM TCEP and 5 μL of 500 mM acetate buffer (pH 5.2) and incubated at room temperature for 1 h. The activated thiolated oligonucleotide was then added to 1.45 mL of 1 mM AuNP solution, followed by incubation at room temperature for 16 h. Subsequently, 15 μL of 500 mM Tris–acetate buffer (pH 8.2) and 150 μL of 1.0 M NaCl were added dropwise to the mixture and mixed well. The mixture was kept in a drawer at room temperature for 24 h. Unbound DNAs and chemicals were removed by centrifugation at 14 000 rpm for 30 min, and the supernatant was discarded. The remaining red pellet was washed three times with 250 μL of 25 mM Tris–acetate (pH 8.0) containing 100 mM NaCl and finally re-dispersed in 500 μL of the same washing buffer containing 8% sucrose. The optical density of the conjugate was measured using a UV-vis spectrometer (Cytation 5 Biotek, Multi-Mode Reader).

Preparation of mesoporous silica particles coated with capture probes

Mesoporous silica particles (MSPs) were prepared according to the Mu, X. *et al.*[45] method with some modifications. Briefly, 0.2355 g of CTAB was dissolved in a mixture of 120 mL of ethanol and 75 mL of Milli-Q water and stirred at 400 rpm. To this solution, 9.975 mL of ammonium hydroxide was added, followed by 1.2 mL of TEOS. Stirring was continued for 4 h. Finally, the mixture was washed 4 times with water and calcined at 500 °C for 6 h. After calcination, the particle has a diameter of around 1 micron, as measured using a Zetasizer (Malvern Panalytical-UK, Nano ZS).

MSPs coated with capture probes (MSPs-capture probes) were prepared according to previous work[46] with some modifications. The method was briefly shown in Fig. 1(A) and demonstrated as follows: 10 mg of MSPs was vigorously sonicated in 1 mL of Milli-Q water. The silica dispersion was then sequentially incubated in 200 μL of PAA and PSS solutions (10 mg mL^{-1} in 0.5 M NaCl). Each polyelectrolyte was allowed to absorb for 30 min at room temperature. Two centrifugation/re-dispersion steps were performed in Milli-Q water to remove excess polyelectrolytes. The resulting polyelectrolyte coated MSPs were dispersed in 1 mL of 1× PBS, pH 7.0. A 10 μL aliquot of avidin (25 mg mL^{-1}) was then added and the suspension was incubated for 90 min under stirring at 37 °C. After that, excess avidin was removed by three centrifugation/re-dispersion steps using 1× PBS, pH 7.4. Then the avidin/MSP was re-dispersed in 1 mL of the same buffer. Finally, 5 μL of 100 μM biotinylated test or control capture probe were added to 500 μL of avidin/MSP solution and the dispersion was incubated for 1 h under stirring at room temperature. The non-binding probe was then

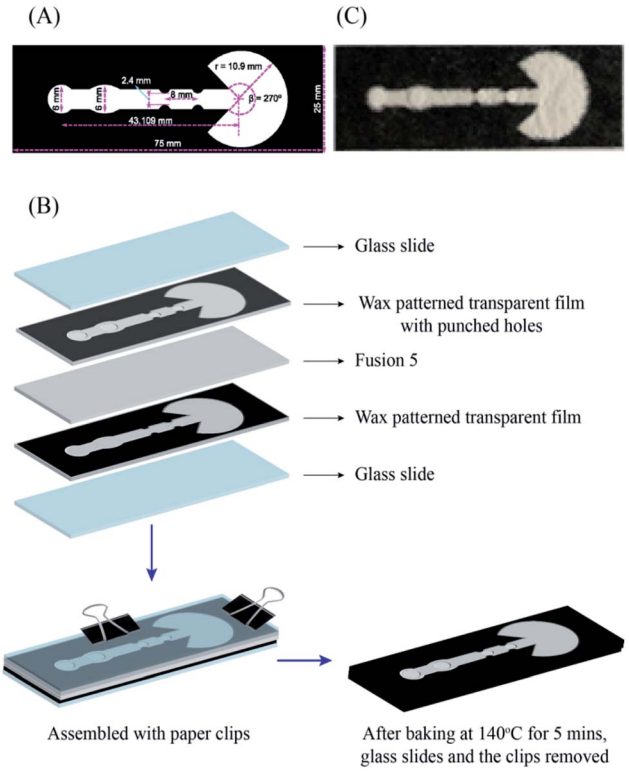

Fig. 1 (A) Showing the developed pattern, designed by Inkscape software and used for fabricating the sensor, (B) schematic representation of the fabrication steps for the wax-patterned fusion 5-based device, and (C) successfully fabricated device.

removed by two centrifugation/re-dispersion steps using 1× PBS, pH 7.4.

Design and fabrication of ACT-Ct-PAD

Microfluidic paper-based analytical devices were designed using Inkscape software and fabricated by wax pattern transfer *via* a transparent film onto a fusion 5 paper substrate. A wax printer with photo-quality mode was used to print wax or solid ink (a mixture of hydrophobic carbamates, hydrocarbons, and dyes that melted at 120 °C) onto printer compatible transparent films. For wax transfer printing, the coated side of the transparent film was printed with wax. For the top film, four circular holes (4.5 mm in diameter for the sample and conjugate areas and 3 mm for the test and control zones) were punched using a hole punch. Two mirror image wax-printed transparent films (one with punched holes and the other without holes) were placed with their wax-patterned side in contact with the paper substrate in a way that they sandwich the substrate. Glass slides were used as a rigid support for holding the substrate and wax-printed films together during heating. A set of four binder clips (one on each side and two in the interior region) held the assembly of the transparent films and substrate, all sandwiched by the glass slides. The assembly was heated in an oven set to 140 °C for 5 min. The fabricated device has a length of 75 mm and a width of 25 mm.

Following the preparation of the device, 7 μL of a AuNPs-DNA label was dispensed on the conjugate area and dried in a silica box at room temperature for 1 h. 1 μL of the MSP-test capture probe and MSP-control capture probe were dispensed on the test and control zones, respectively. The dispensed bio-conjugate is allowed to dry in a silica box for 30 min at room temperature. The obtained ACT-Ct-PAD devices were stored in a silica box at room temperature until use.

Nucleic acid detection based on ACT-Ct-PAD

75 μL of an aliquot of oligonucleotide solutions (or heated PCR products) were applied to the sample area of the ACT-Ct-PAD. Once the solution wicked completely to the absorbent area, the assay was considered complete. The assay duration was monitored with a digital timer. The assay was then interpreted by visual analysis of the colorimetric results and by analysis of images captured with a smartphone camera, after 15 min of dropping the sample.

The captured images were analysed using ImageJ software.[47] First, the images were inverted to grey scale and then the region of interest (ROI) was defined as follows: 23 pixels in diameter for test and control spots and 18 × 18 pixels for the background area (the channel between the test and control spots). The mean inverted grey scale intensity of the background was used to normalize the intensities of the test and control spots. The normalized signal of the device was computed according to the following equation: (normalized signal (T/C) = test − background/control − background).

The selectivity and interference from other non-target oligonucleotides were tested by applying non-complementary DNA from two other *Colletotrichum* species (*C. scovillei* and *C. gloeosporioides* species complexes) and from different fungal genera in the sample solution with and without the *C. truncatum* target DNA. The stability of the prepared device was repeatedly tested during 4 months of storage at room temperature.

DNA extraction method

For DNA extraction, fungal mycelium was harvested with forceps from malt broth (MB; malt extract 20 g L^{-1}) culture and suspended in extraction buffer consisting of 0.25 M EDTA, 2.5% SDS, and 0.5 M Tris, pH 9. For DNA extraction from chili seeds, 50 mg of seeds of interest were homogenized in 200 μL of extraction buffer for 1 min using an automated homogenizer.

To this suspension, 200 μL of extraction buffer was then added and incubated at 65 °C for 5 min, followed by the addition of 192 μL of extraction buffer. After that, 200 μL of the mixture solution of chloroform: isoamyl alcohol (24 : 1, v/v) was added and incubated on ice for 5 min and then centrifuged at 14 000 g for 10 min. 400 μL of isopropanol was added to the clear supernatant obtained to precipitate nucleic acid. The tube was centrifuged at 14 000 g for 5 min and the isopropanol layer was discarded. The pellet was washed twice with 70% ethyl alcohol. After washing, the genomic DNA was resuspended in 25 μL nuclease-free water and stored at −20 °C.

PCR amplification method

PCR was performed in a 25 μL reaction mixture containing 0.25 mM dNTPs, 0.5 U Taq polymerase, 0.1 μM of each primer

and 100 ng μL^{-1} of mycelium DNA template or 50 ng μL^{-1} of spore DNA template. The PCR cycle consisted of 1 cycle of 5 min at 95 °C, 30 cycles of 30 s at 95 °C, 30 s at 62 °C, and 30 s at 72 °C and a final cycle of 72 °C for 5 min.

Real sample testing

After extracting genomic DNA from the desired seeds, the amplified PCR product (96 bp) was then obtained. 10 μL of the PCR product were diluted in 65 μL of 0.01 M PBS, pH 7.4, followed by heat denaturation in a boiling water bath at 95 °C for 5 min and immediately applied to the sample area of ACT-Ct-PAD, such that the samples were still warm. The images of tested ACT-Ct-PAD device were captured by using a smartphone and they were analyzed using ImageJ software as described previously.

Results and discussion

The working principle of the device for the detection of *C. truncatum* based on DNA hybridization was shown in Fig. 1(B). The designed device was composed of sample, conjugate, detection (including test and control zones) and absorbent areas. Test capture probe coated MSPs specific to the *C. truncatum* target DNA were dispensed on the test zone. On the control zone, control capture probe coated MSPs were immobilized for direct hybridization with control DNAs attached to AuNPs. At the same time, AuNP-DNA label was stored in the conjugate zone for hybridization with *C. truncatum* target DNA. Detection DNAs were attached to the surface of AuNPs through the covalent bond between thiol and Au. Here, the control DNA was used for hybridization with pre-immobilized control capture probe coated MSPs on the control zone. After introduction of the sample solution containing the target DNA onto the sample area, the solution migrated towards the absorbent area by capillary action. When the sample solution passed through the conjugate area, the target DNA hybridized with the detection DNA attached to the surface of AuNPs to form a DNA hybridization complex, which continued to flow along the device. When this complex reached the test zone, the complex was captured by the test capture probe coated MSPs that were pre-immobilized on the test zone. Consequently, sandwich DNA hybridization complexes were formed on the test zone. Finally, the excess conjugate continued to migrate, and it was captured by the control capture probe coated MSPs in the control zone.

Design of ACT-Ct-PAD

The wax-patterned device was designed using Inkscape software to accommodate DNA hybridization-based detection. The pattern was composed of a sample area, conjugate storage area, two constriction structures positioned directly upstream of the test and control zones, and a fan-shaped waste area (adapted from Mendez *et al.*[48]). The design is superior to the conventional lateral flow strip as the constriction structures function to increase the fluidic resistance of the channel and reduce the flow rate of the sample through the areas, extending the reaction time of the hybridization assay. Furthermore, the immobilized capture DNAs occupied an area smaller than the channel's width; hence, narrowing the channel just before the test and control zones forces the hybridization complex to come into contact with the capture DNAs.

Printing wax directly on Fusion 5 paper is inappropriate due to many reasons: (i) the texture of Fusion 5 is cotton-like and very delicate, causing indistinct wax-patterning, (ii) such delicate paper can break inside the printer causing considerable damage, and (iii) according to the manufacturer's specifications, the thickness of Fusion 5 paper is 0.37 mm (2-fold that of Whatman grade 1 chromatography paper). This thickness is impenetrable by the wax provided by this printer. To overcome this problem, we applied wax-pattern transfer *via* a transparent film.

The dimensions of the pattern designed for fabricating the device were shown in Fig. 1(A). The device was fabricated in two simple steps by printing the desired pattern on two pieces of the transparent film and then transferring the pattern onto Fusion 5 paper as shown in Fig. 1(B). The front and back sides of the wax-patterned Fusion 5 sensor were shown in the ESI Fig. S2(A).† The back side, where the Fusion 5 surface is unsmooth, shows an indistinct signal. In contrast, the front side Fusion 5 surface is smooth, providing a sharp signal. The dimensions of different parts of the fabricated device were reduced compared to those of the designed pattern (Fig. S2(B)†).

Fusion 5 paper is a type of glass fiber. It is non-protein binding under normal test conditions; therefore, it is difficult to immobilize DNA–streptavidin directly on the paper. Accordingly, we have used MSPs as a carrier for capture probes, which will increase the surface area and improve the hybridization efficiency. Application of the wax-patterned fusion 5 sensor in this study eliminates the need for pre-treatment steps required for other types of paper. The localization of the particles deposited onto the paper was confirmed by using dye doped MSPs tested with flowing buffer (Fig. S2†).

Detection of oligonucleotides on ACT-Ct-PAD

As shown in Scheme 1(B), the efficiency of hybridization duplex formation is a function of several factors. Thus, to improve the sensitivity of the ACT-Ct-PAD, the buffer composition, MSP-capture probe concentration, and AuNPs-DNA label concentration were investigated using oligonucleotides. The ESI (Fig. S3†) shows that the optimized conditions for ACT-Ct-PAD were attained by using 0.01 M PBS, pH 7.4 as a running buffer, 160 μg μL^{-1} of MSP-capture probe, and concentration of AuNPs-DNA at OD = 7.5.

Under these optimized conditions, different concentrations of the 69 mer sequence of the synthetic target DNA common to the actin gene of *C. truncatum* (0 to 75 nM) were tested using the ACT-Ct-PAD. Images of the device captured after 10–15 min of reaction using a smartphone (Fig. S4†) were analyzed. The error from the image capturing time and lighting conditions can be eliminated by subtracting the background.[44] The normalized intensity (T/C) was plotted against the different concentrations of the target DNA, as shown in Fig. 2. The results showed

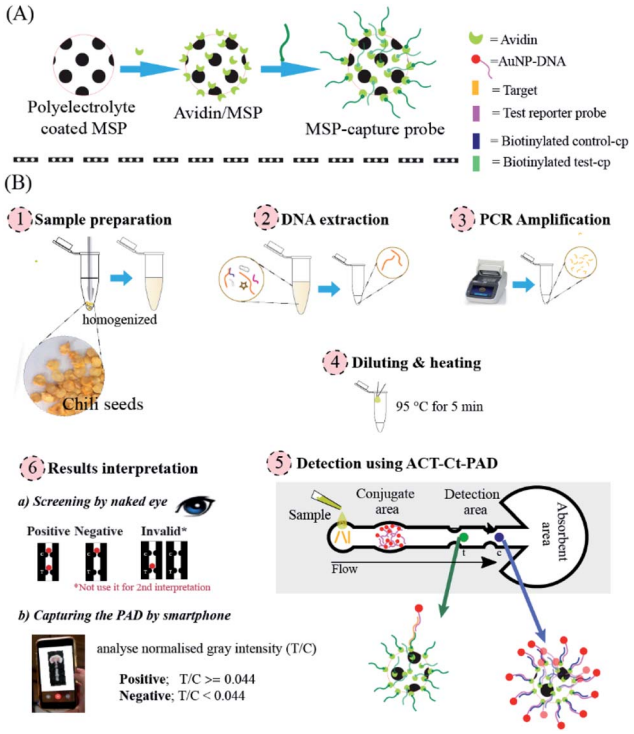

Scheme 1 (A) Schematic representation of the preparation of the mesoporous silica particle (MSP) – capture probe conjugate through layer by layer coating and (B) the detection work flow of *Colletotrichum truncatum* from chili seeds using ACT-Ct-PAD for the actin gene sequence.

a linear relationship between the normalized intensity and concentration of *C. truncatum* DNA ((T/C) = 0.6078x(log c [pM]) − 1.3894 with $r^2 = 0.99$, $n = 152$). The increasing concentrations of the target DNA showed increasing signal intensity for a linear response of 0.5 to 75 nM. The limit of detection (LOD) was calculated using the following equation; $\dot{x} + 3\sigma$, where $\dot{x}$ is the mean response to DNA-free buffer and σ is the standard deviation of that response. Determination of nineteen assays in the absence of DNA gave a cut-off value of 0.044 from normalized grey intensity (used to distinguish between positive and negative results), in which the LOD was calculated to be about 232 pM. This corresponds to the detection of 17.42 femtomoles of the DNA in 75 μL of the target solution.

The selectivity of ACT-Ct-PAD was studied using 5 and 50 nM of oligonucleotides designed from the actin gene sequence of *C. scovillei* (Cs) and *C. gloeosporioides* (Cg) and other fungi including *A. niger* and *A. alternata*, frequently found in chili pepper seeds and fruits (Fig. 3). The results indicated that the ACT-Ct-PAD showed high selectivity for *C. truncatum*. When the target and non-target DNA were mixed and applied to ACT-Ct-PAD, it showed selectivity for the desired target only without any interference.

The stability of ACT-Ct-PAD stored in the dark and low humidity at room temperature (≈25 °C) was investigated and the results indicated that the normalized intensity of the PAD was not significantly changed during the 4 months of storage.

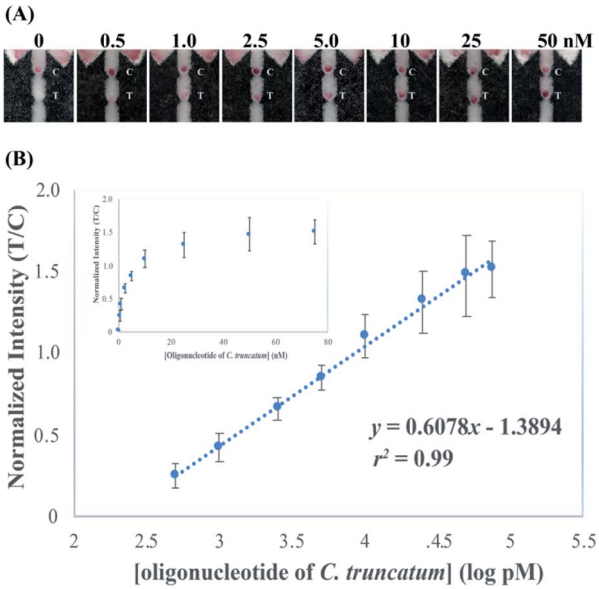

Fig. 2 (A) Images captured with a smartphone, for the detection area of devices tested with 0–50 nM of *C. truncatum* oligonucleotides (B) normalized intensity (T/C) plotted against different concentrations of target oligonucleotides between 0 and 75 nM (converted to the log of pM) in 1× PBS, pH 7.4, ($n = 19$).

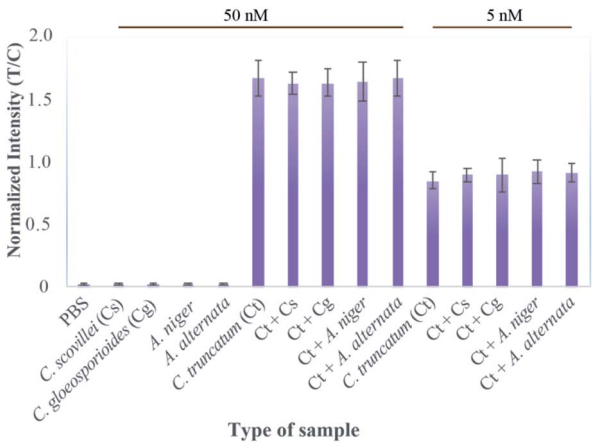

Fig. 3 Selectivity of the sensor to *C. truncatum* (Ct) DNA and the absence of signals for DNA from other *Colletotrichum* species (Cs = *C. scovillei* and Cg = *C. gloeosporioides* species complex) and DNA from other fungal genera (*A. niger* = *Aspergillus niger* and *A. alternata* = *Alternaria alternata*). Tested using 5 and 50 nM of target DNA and 1× PBS as the control ($n = 19$).

Testing of infected seeds

This study described the development of ACT-Ct-PAD for the specific detection of *Colletotrichum truncatum* in chili pepper seeds. A key requirement for successful detection of specific microorganisms using PCR-based assay is the adequate selection of genetic markers for designing highly specific primers.[49] Consequently, we have designed a pair of species-specific primers from the actin gene.[10] Using these primers, a specific 96 bp PCR product was successfully obtained for all isolates of *C. truncatum*.

To validate the ACT-Ct-PAD, PCR products obtained by using varying concentrations of *C. truncatum* genomic DNA (extracted from mycelium) were used to test the device (Fig. 4). A negative control (non-template PCR product) was included in the reactions and its response was negative.

The real sample testing was evaluated by spiking healthy seeds with spores of *C. truncatum*. Conventionally, the qualitative detection was performed using electrophoresis. However, in this study, ACT-Ct-PAD was used for quantitative detection. The results derived from detecting two batches of PCR products using ACT-Ct-PAD were shown in Table 2. The normalized signal (T/C) value for healthy seeds was lower than the cut-off value. Therefore, it showed a negative result. On the other hand, the T/C values for Ct-infected seeds could be calculated to be 685 pM, using the linear equation in Fig. 2. The precision of the determination of PCR products from Ct-infected seeds using ACT-Ct-PAD was 2.68%.

The sensitivity of ACT-Ct-PAD and gel electrophoresis for detecting PCR products was almost the same;[10] however, ACT-Ct-PAD can provide a simple and quantitative detection of *C. truncatum* PCR products within 15 min and without the need for expensive equipment. The sensitivity of the device can be improved by using multi-copy genetic markers to design primers and probes, since the actin gene is a single copy. Methods such as those using a gold nanoparticle two-probe detection system[50] and gold-latex[51] can further improve the sensitivity. Further improvements in this protocol can be achieved by applying techniques such as recombinase polymerase amplification (RPA) to replace the PCR technique, which requires specialized equipment and a skilled operator.

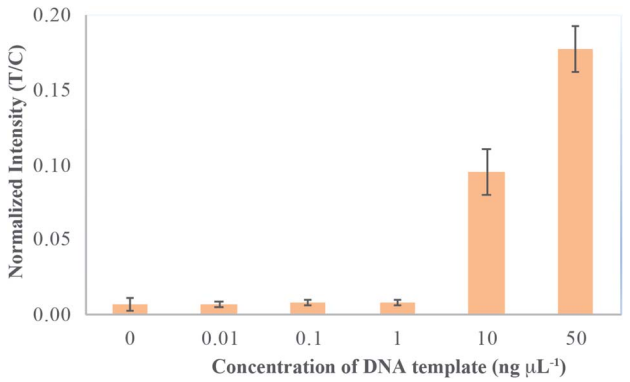

Fig. 4 The relationship between various concentrations of template genomic DNA (used for PCR) and normalized intensity (T/C) of the device image captured with a smartphone camera ($n = 19$).

Table 2 The relative standard deviation (% RSD) of healthy seeds and Ct-infected seeds analysed using ACT-Ct-PAD

PCR		Ct-infected seeds	Healthy seeds
Batch 1	T/C	0.327 ± 0.005	0.012 ± 0.002
	% RSD	1.52	
Batch 2	T/C	0.333 ± 0.011	0.013 ± 0.001
	% RSD	2.68	
Total	T/C	0.33 ± 0.009	0.012 ± 0.002
	% RSD	2.68	

Conclusions

The success of wax transfer and penetration through Fusion 5 paper allowed the fabrication of DNA biosensors for *C. truncatum* detection. The non-protein binding nature of Fusion 5 also eliminated the need for laborious blocking steps common to all cellulose based devices. The diagnostic test described herein was proved to be reproducible with a detection limit down to the femtomole level. It could detect the PCR products of DNA extracted from infected chili pepper seeds. Moreover, the test was simple and rapid (as it can be performed in 15 min) and the results can be easily interpreted. The wax-patterned Fusion 5 platform is capable and convenient for the future development of DNA and immuno-based sensors.

Author contributions

A. O. A. carried out the experiment and wrote the manuscript with support from B. T. T., P. R., and W. S. B. T. T. designed the device and figures using software. A. O. A. and P. R. conceived the original idea. P. R. and W. S. supervised the project.

Conflicts of interest

There is no conflict of interest to declare.

Acknowledgements

We gratefully acknowledge the financial support provided by King Mongkut's University of Technology Thonburi through the "KMUTT 55th Anniversary Commemorative Fund". We also thank Dr Sawita Suwannarat for providing all *Colletotrichum* isolates and giving valuable comments.

References

1 R. Dean, J. A. Van Kan, Z. A. Pretorius, K. E. Hammond Kosack, A. Di Pietro, P. D. Spanu, J. J. Rudd, M. Dickman, R. Kahmann, J. Ellis and G. D. Foster, *Mol. Plant Pathol.*, 2012, **13**(4), 414–430, DOI: 10.1111/j.1364-3703.2011.00783.x.

2 D. D. de Silva, J. Z. Groenewald, P. W. Crous, P. K. Ades, A. Nasruddin, O. Mongkolporn and P. W. J. Taylor, *IMA Fungus*, 2019, **10**, 8, DOI: 10.1186/s43008-019-0001-y.

3 M. Kamle, B. K. Pandey, P. Kumar and M. Kumar, *J. Plant Pathol. Microbiol.*, 2013, **4**(6), 1000184, DOI: 10.4172/2157-7471.1000184.

4 B. Tibebu and B. Nuh, *Afr. J. Biotechnol.*, 2019, **18**(29), 797–807, DOI: 10.5897/AJB2018.16591.

5 X. Yang, U. Hameed, A. F. Zhang, H. Y. Zang, C. Y. Gu, Y. Chen and Y. L. Xu, *Sci. Rep.*, 2017, **7**, 40954, DOI: 10.1038/srep40954.

6 S. Wang, W. Ye, Q. Tian, S. Dong and X. Zheng, *Australas. Plant Pathol.*, 2017, **46**, 493–498, DOI: 10.1007/s13313-017-0511-2.

7 S. Pecchia and D. Da Lio, *J. Microbiol. Methods*, 2018, **151**, 118–128, DOI: 10.1016/j.mimet.2018.06.010.
8 A. O. Abdelrazig, S. Suwannarat, P. Rijiravanich and W. Surareungchai, *Eur. J. Plant Pathol.*, 2020, **158**, 571–582, DOI: 10.1007/s10658-020-02103-9.
9 S. Mosca, M. G. Li Destri Nicosia, S. O. Cacciola and L. Schena, *PLoS One*, 2014, **9**(12), e114031, DOI: 10.1371/journal.pone.0114031.
10 A. O. Abelrazig, N. Siriyod, S. Suwannarat, P. Rijiravanich and W. Surareungchai, *Eur. J. Plant Pathol.*, 2021, under revision.
11 P. Gutiérrez, M. S. Yepes, J. F. A. Restrepo, K. V. Berrouet and M. M. Montoya, *Trop. Plant Patho.*, 2014, **39**(4), 275–283, DOI: 10.1590/S1982-56762014000400002.
12 S. Scibetta, L. Schena, A. Abdelfattah, S. Pangallo and S. O. Cacciola, *Phytobiomes J.*, 2018, **2**(4), 225–236, DOI: 10.1094/PBIOMES-02-18-0009-R.
13 L. Kiss, *Proc. Natl. Acad. Sci.*, 2012, **109**(27), E1811, DOI: 10.1073/pnas.1207143109.
14 U. Damm, P. F. Cannon, J. H. Woudenberg and P. W. Crous, *Stud. Mycol.*, 2012, **73**(1), 37–113, DOI: 10.3114/sim0010.
15 H. M. Daniel and W. Meyer, *Int. J. Food Microbiol.*, 2003, **86**(1–2), 61–78, DOI: 10.1016/S0168-1605(03)00248-4.
16 V. Reeb, F. Lutzoni and C. Roux, *Mol. Phylogenet. Evol.*, 2004, **32**(3), 1036–1060, DOI: 10.1016/j.ympev.2004.04.012.
17 L. Huang, J. Wang, Q. Wang, D. Tang and Y. Lin, *Mikrochim. Acta*, 2020, **187**(10), 563, DOI: 10.1007/s00604-020-04546-7.
18 Z. Lin, S. Lv, K. Zhang and D. Tang, *J. Mater. Chem. B*, 2017, **5**(4), 826–833, DOI: 10.1039/C6TB03042D.
19 S. Lv, Y. Tang, K. Zhang and D. Tang, *Anal. Chem.*, 2018, **90**(24), 14121–14125, DOI: 10.1021/acs.analchem.8b04981.
20 Z. Qiu, J. Shu and D. Tang, *Anal. Chem.*, 2017, **89**(9), 5152–5160, DOI: 10.1021/acs.analchem.7b00989.
21 Z. Yu, Y. Tang, G. Cai, R. Ren and D. Tang, *Anal. Chem.*, 2018, **91**(2), 1222–1226, DOI: 10.1021/acs.analchem.8b04635.
22 D. M. Cate, J. A. Adkins, J. Mettakoonpitak and C. S. Henry, *Anal. Chem.*, 2015, **87**(1), 19–41, DOI: 10.1021/ac503968p.
23 S. Abarghoei, N. Fakhri, Y. S. Borghei, M. Hosseini and M. R. Ganjali, *Spectrochim. Acta, Part A*, 2019, **210**, 251–259, DOI: 10.1016/j.saa.2018.11.026.
24 N. Fakhri, S. Abarghoei, M. Dadmehr, M. Hosseini, H. Sabahi and M. R. Ganjali, *Spectrochim. Acta, Part A*, 2020, **227**, 117529, DOI: 10.1016/j.saa.2019.117529.
25 K. S. Prasad, Y. Abugalyon, C. Li, F. Xu and X. Li, *Analyst*, 2020, **145**, 5113–5117, DOI: 10.1039/D0AN00704H.
26 M. Gutierrez-Capitan, A. Baldi and C. Fernandez-Sanchez, *Sensors*, 2020, **20**(4), 967, DOI: 10.3390/s20040967.
27 S. W. Loo and T. S. Pui, *Sensors*, 2020, **20**(17), 1854, DOI: 10.3390/s20071854.
28 L. Ge, J. Yu, S. Ge and M. Yan, *Anal. Bioanal. Chem.*, 2014, **406**(23), 5613–5630, DOI: 10.1007/s00216-014-7756-1.
29 M. Mirasoli, M. Guardigli, E. Michelini and A. Roda, *J. Pharm. Biomed. Anal.*, 2014, **87**, 36–52, DOI: 10.1016/j.jpba.2013.07.008.
30 S. R. Chinnadayyala, J. Park, H. T. N. Le, M. Santhosh, A. N. Kadam and S. Cho, *Biosens. Bioelectron.*, 2019, **126**, 68–81, DOI: 10.1016/j.bios.2018.10.038.
31 E. M. Gross, H. E. Durant, K. N. Hipp and R. Y. Lai, *ChemElectroChem*, 2017, **4**(7), 1594–1603, DOI: 10.1002/celc.201700426.
32 H. Liu, X. Zhou, Q. Shen and D. Xing, *Theranostics*, 2018, **8**(8), 2289–2299, DOI: 10.7150/thno.23483.
33 F. Wang, Y. Liu, C. Fu, N. Li, M. Du, L. Zhang, S. Ge and J. Yu, *Anal. Chem.*, 2021, **93**, 1702–1708, DOI: 10.1021/acs.analchem.0c04307.
34 J. Qi, B. Li, X. Wang, Z. Zhang, Z. Wang, J. Han and L. Chen, *Sens. Actuators, B*, 2017, **251**, 224–233, DOI: 10.1016/j.snb.2017.05.052.
35 M. Sarwar, J. Leichner, G. M. Naja and C. Z. Li, *Microsyst. Nanoeng.*, 2019, **5**, 56, DOI: 10.1038/s41378-019-0096-8.
36 A. T. Singh, D. Lantigua, A. Meka, S. Taing, M. Pandher and G. Camci-Unal, *Sensors*, 2018, **18**(9), 2838, DOI: 10.3390/s18092838.
37 S. Ahmed, M. P. Bui and A. Abbas, *Biosens. Bioelectron.*, 2016, **77**, 249–263, DOI: 10.1016/j.bios.2015.09.038.
38 A. K. Yetisen, M. S. Akram and C. R. Lowe, *Lab Chip*, 2013, **13**(12), 2210–2251, DOI: 10.1039/C3LC50169H.
39 J. M. Goddard and J. H. Hotchkiss, *Prog. Polym. Sci.*, 2007, **32**(7), 698–725, DOI: 10.1016/j.progpolymsci.2007.04.002.
40 S. Hosseini, F. Ibrahim, I. Djordjevic and L. H. Koole, *Analyst*, 2014, **139**(12), 2933–2943, DOI: 10.1039/C3AN01789C.
41 X. Jiang and P. B. Lillehoj, *Analyst*, 2021, **146**(3), 1084–1090, DOI: 10.1039/D0AN02073G.
42 R. H. Tang, L. N. Liu, S. F. Zhang, X. C. He, X. J. Li, F. Xu, Y. H. Ni and F. Li, *Microchim. Acta*, 2019, **186**, 521, DOI: 10.1007/s00604-019-3626-z.
43 R. Cao, L. Guan, M. Li, J. Tian and W. Shen, *Sensing and Bio-Sensing Research*, 2015, **6**, 13–18, DOI: 10.1016/j.sbsr.2015.09.002.
44 M. H. Prabowo, S. Chatchen, P. Rijiravanich, K. Limkittikul and W. Surareungchai, *Anal. Bioanal. Chem.*, 2020, **412**(12), 2915–2925, DOI: 10.1007/s00216-020-02527-6.
45 X. Mu, C. L. Wu, J. P. Lai, J. B. Chen, J. S. Zheng, C. Li and Y. B. Zhao, *Chin. Sci. Bull.*, 2011, **56**(31), 3242–3246, DOI: 10.1007/s11434-011-4727-1.
46 N. Cheeveewattanagul, P. Rijiravanich, W. Surareungchai and M. Somasundrum, *J. Electroanal. Chem.*, 2016, **779**, 61–66, DOI: 10.1016/j.jelechem.2016.05.002.
47 C. A. Schneider, W. S. Rasband and K. W. Eliceiri, *Nat. Methods*, 2012, **9**(7), 671–675, DOI: 10.1038/nmeth.2089.
48 S. Mendez, E. M. Fenton, G. R. Gallegos, D. N. Petsev, S. S. Sibbett, H. A. Stone, Y. Zhang and G. P. Lopez, *Langmuir*, 2010, **26**(2), 1380–1385, DOI: 10.1021/la902470b.
49 A. Kuzdralinski, A. Kot, H. Szczerba, M. Nowak and M. Muszynska, *J. Mol. Microbiol. Biotechnol.*, 2017, **27**(3), 175–189, DOI: 10.1159/000477544.
50 S. Oaew, N. Karoonuthaisiri and W. Surareungchai, *Biosens. Bioelectron.*, 2009, **25**(2), 435–441, DOI: 10.1016/j.bios.2009.07.031.
51 Y. Matsumura, Y. Enomoto, M. Takahashi and S. Maenosono, *ACS Appl. Mater. Interfaces*, 2018, **10**(38), 31977–31987, DOI: 10.1021/acsami.8b11745.